

The theory of quark confinement^{*†}

V. N. Gribov

Landau Institute for Theoretical Physics, Moscow

and

Research Institute for Particle and Nuclear Physics, Budapest

and

Institut für Theoretische Kernphysik der Universität Bonn

Abstract

This is the second of the two last papers by V. N. Gribov concluding his 20 year long study of the problem of quark confinement in QCD. In this paper the analytic structure of quark and gluon Green's functions is investigated in the framework of the theory of confinement based on the phenomenon of supercritical binding of light quarks. The problem of unitarity in a confining theory is discussed. The write-up remained unfinished and so it is presented here. The author was planning to emphasise the link between the electro-weak and strong interactions, and in particular the rôle of pions (Goldstone bosons) in confinement, to present an explicit solution for bound states, and to write down an analytic model for quark and gluon Green's functions corresponding to confinement.

1 Introduction¹

Almost ten years ago [1] I proposed a hypothesis according to which quarks and gluons are confined due to the existence of light quarks (u and d) with Compton wavelengths much larger than the radius of strong interaction defined by λ_{QCD} . The essence of this hypothesis is the supercritical phenomenon which is well-known in QED where it is the following. If there exists a heavy nucleus of radius R with charge Z exceeding a critical value Z_{cr} (which is of the order of 137), the vacuum of the light charged fermions (electrons) becomes unstable

^{*} The work was completed in Bonn under the Humboldt Research Award Program.

[†] The text was prepared for publication by Yu. Dokshitzer, C. Ewerz, and J. Nyiri, with help from J. Bartels, A. Kaidalov, A. Mueller and A. Vainshtein.

¹The author intended to rewrite this Introduction. In the present form it corresponds to the Introduction to the Lecture given by V. N. Gribov at the 34th International School of Subnuclear Physics in Erice, Italy, in 1996 [7].

due to the process of (e^-, e^+) pair creation. The negative component of the pair, the electron, falls into the heavy charge and the positive component goes to infinity. The condition for this phenomenon to occur is that the Compton wave length $1/m$ of the electron has to be much larger than the radius of the heavy charge:

$$\alpha\sqrt{Z^2 - Z_{cr}^2} \ln(mR) > \pi. \quad (1.1)$$

The electron which falls into the centre forms together with the source Z an ion of charge $Z_1 = Z - 1$. If $Z - 1 > Z_{cr}$, this process will continue until the vacuum becomes stable i.e. when $Z_n = Z - n$ becomes less than the critical charge.

From the point of view of the Dirac equation the falling electron has negative energy. On the other hand, the supercritical ion with $Z_n < Z_{cr}$ is stable because of the Pauli principle. Indeed, the electron cannot leave the ion, since all negative energy states outside it are occupied.

In QCD this phenomenon can occur since, due to asymptotic freedom, the colour charge can reach the critical value for any object. Let us suppose that two heavy quarks are created with opposite colours. The gluonic vacuum polarisation increases the colour charges of the

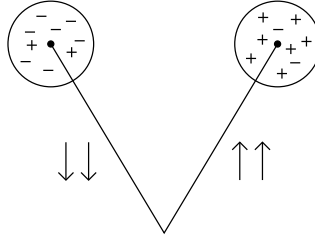


Figure 1:

quarks (see Fig. 1). When these colour charges become large enough, light antiquarks start to fall onto the heavy quark. However, the bound state formed by a light antiquark and a heavy quark will be very different from the bound states which appeared in QED. In QED we had an ion with a charge $Z - 1$. In QCD the corresponding state can be colourless. The difference is due to the fact, that while the large colour charge of the heavy quark results from gluonic vacuum polarisation, the bound state is formed by two particles the total charge of which equals zero, and this charge cannot be changed by vacuum polarisation. This phenomenon can be called quantum screening. Formally it means that the heavy quark q_h is unstable and has to decay into a meson and a light quark q_l

$$q_h \rightarrow M + q_l. \quad (1.2)$$

This case — the confinement of the heavy quark — is relatively simple and almost independent of the properties of the light quark [2]. The problem of the light quark is more difficult. At first sight it is not clear whether the "falling into the centre" and the formation of a supercritical state can occur in the system of a light quark and a light antiquark. It was shown [3], however, that indeed the critical phenomenon exists in the light $q\bar{q}$ system.

Moreover, the critical coupling constant is proven to be sufficiently small:

$$\frac{\alpha_{cr}}{\pi} = \left(1 - \sqrt{\frac{2}{3}}\right) \cdot \frac{3}{4} \simeq 0.14. \quad (1.3)$$

There is an even more complicated question: what kind of states can be formed as a result of this phenomenon? If the appearing new state is a normal meson, the "falling into the centre" leads to

$$q_l \rightarrow M + q_l \quad (1.4)$$

instead of (1.2). Equation (1.4) can be satisfied if there are not only positive energy quarks q_+ but also negative energy quarks q_- . This result, although it looks very strange, is not unexpected. Indeed, we already learned in QED that particles which fall into the centre correspond to the negative energy solution of the Dirac equation.

To resolve the problem of the negative energy states, Dirac supposed that they are all occupied and therefore not observable. The necessity to consider now both the positive and negative solutions of the Dirac equation means only that Dirac's hypothesis is not always true. If the interaction is strong enough, there is another possibility: negative energy states might be only partly occupied and positive energy states only partly empty. This is, however, not in contradiction with the absence of negative energy particles in the real world if stable supercritical bound states (mesons) exist since in this case both the positive and negative energy quarks will be unstable:

$$q_+ \rightarrow M + q_-$$

$$q_- \rightarrow M + q_- q_- \bar{q}_- \quad (1.5)$$

and, consequently, unobservable.

From the point of view of the fermionic spectrum in the vacuum, (1.5) means the following. In the case of weak interactions, the fermionic spectrum has a structure corresponding to Fig. 2. All levels above $q_0 = \sqrt{\vec{q}^2 + m_f^2}$ are empty, and the levels below $q_0 = -\sqrt{\vec{q}^2 + m_f^2}$ are occupied. If the interaction is stronger than critical, quark-antiquark pairs are present in the vacuum, and the spectrum has a structure which roughly corresponds to Fig. 3: all levels are occupied in the shaded regions and empty in the unshaded ones. In terms of condensed matter physics, the curves $q_0 = \pm\sqrt{\vec{q}^2 + m_f^2}$ correspond to the Fermi surface. The change in the number of constituents in the theory is also natural from the point of view of the physics of condensed matter. In a theory with weak coupling we had two constituents q and \bar{q} ; a theory with supercritical coupling contains four states q_+ , q_- , \bar{q}_+ and \bar{q}_- . In non-relativistic physics there are only particles (electrons) and no antiparticles. But in a conductor we have particles and holes, and holes are negative energy states (counting the energy of the holes from zero and not from the Fermi energy as it is usually done).

In a relativistic theory it is impossible to add a constant to the energy of particles, and therefore we are forced to talk about negative energy states which exist only inside our matter (vacuum).

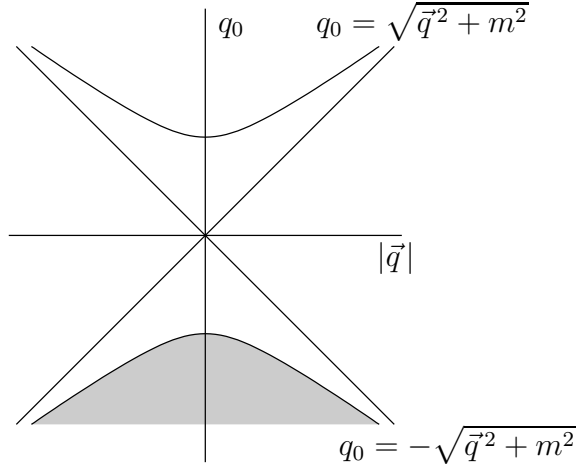


Figure 2:

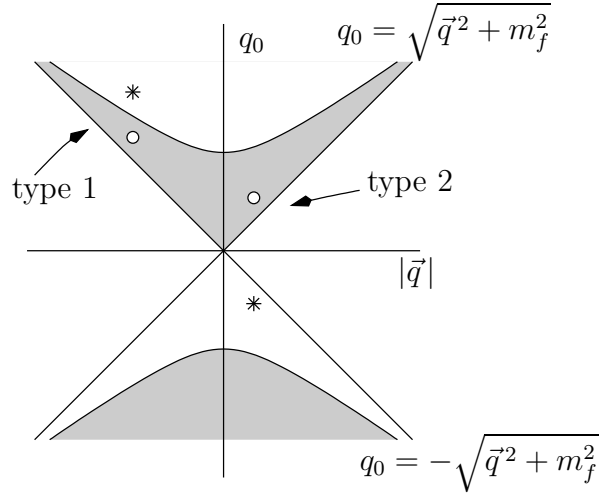


Figure 3:

This unusual quark spectrum has been discussed for several years. Still, I have not been able to formulate a constructive theory because I have not understood what meson had to be introduced as a supercritical bound state. From the structure of the spectrum shown in Fig. 3 it is clear that there have to be different types of excitations corresponding to different types of mesons. It is natural to identify hole-particle excitations of the type 1 near the Fermi surface with mesons like ρ , ω etc. Hole-particle excitations near the light cone can be identified with the a_0 and f_0 mesons [4] and also with η' . But all these mesons do not look like natural candidates for the lowest supercritical bound states. Only recently did I recognise that there are strong reasons to believe that the pseudoscalar octet, and the π -meson in particular, are in fact the lowest supercritical bound states. Most of these reasons are connected with the discussion of the nature of the π -meson state which I presented in [5].

As I have said before, the supercritical atom in QED is not a usual Bohr-type atom, containing a definite number of electrons. Rather, it is a collective state in which only the electron density is localised around the heavy charge, and only at large distances (much

larger than the atomic radius) it looks like a state with a definite electron number. A quasi-Goldstone state like a π -meson with a finite mass has the same properties. At short distances (distances less than λ_{QCD}) it can be considered as a collective state of the type $q_l \bar{q}_l - q_r \bar{q}_r$ (divergence of the pseudovector current; q_l and q_r stand for left-handed and right-handed quarks), whereas at large distances it is the two-particle state $q_l \bar{q}_r - q_r \bar{q}_l$. Accepting this identification with the π -meson as the lowest supercritical state by introducing it explicitly in the equation for the quark Green function (which will be discussed in the next part of the lecture), it proves possible to find a solution for this Green function which has properties corresponding to the spectrum in Fig. 3. This solution has two complex poles as functions of energy in the complex energy plane in accordance with the two types of quarks (constituent and current) we have discussed. It has no pole on the real axis which guarantees that quarks as propagating states do not exist. It has a soft singularity when $q^2 \rightarrow 0$, reflecting the fact that quark currents exist in the region where the hadrons are created. It is important to stress that in all these considerations I assume the coupling constant α is saturated at a value not much larger than α_{cr} . Quark masses corresponding to the positions of the two complex poles m_{\pm} are of the order of

$$m_{\pm} \sim \lambda_{\text{QCD}} \exp \left(-\frac{C_{\pm}}{\sqrt{\alpha - \alpha_{cr}}} \right).$$

The solution for the Green's function is self-consistent if the π -meson mass is close to m_- . This means that at least in the case when α is not very large, the π -meson mass is defined by strong interaction dynamics. This result contradicts the usual point of view according to which the π -meson mass squared is the product of the bare quark mass m_0 defined by weak interactions and the condensate density $\langle \bar{\Psi} \Psi \rangle / f_{\pi}^2$ defined by strong interactions.

In what follows I will explain what type of equations have to be written and solved in order to come to the conclusion I have stated and to calculate quantities which have not been analysed until now. For example, quark-gluon vertices and the gluon Green's function have not been calculated yet. It is clear, however, that the gluon Green's function we obtain will also have a complex singularity due to the gluon decay into a $q\bar{q}$ pair. Consequently, the gluon will also be confined. Equations for hadronic amplitudes can also be written constructively if α is not very large. It can be shown that if the quark Green's function has properties as described above, the hadronic amplitude will have no singularities connected with intermediate $q\bar{q}$ states, but will have singularities related to the π -meson thresholds. The fact that the π -meson is included intrinsically in the equation for the quark Green's function and has a mass of the order of m_- makes this statement much less mysterious than it would look without it.

2 The structure of the confined solution for the Green's function of massless quarks

In the paper [6] we considered the solution for the quark Green's function corresponding to the chiral symmetry breaking. We discussed the importance of including the contribution of the Goldstone boson in the equation. In the present paper we show that this solution

does not necessarily survive in the presence of the Goldstone contribution which, essentially, reflects the softness of the condensate and leads to the existence of a solution which has no poles and which corresponds to confined quarks.

We will accept the equation for the quark Green's function in the form

$$\partial^2 G^{-1}(q) = g(q) \partial_\mu G^{-1}(q) G(q) \partial_\mu G^{-1}(q) - \frac{3}{16\pi^2 f_\pi^2} \{i\gamma_5, G^{-1}(q)\} G \{i\gamma_5, G^{-1}(q)\} \quad (2.1)$$

where $g(q) = \frac{4}{3} \frac{\alpha}{\pi}$ is supposed to behave like in [6] (see Fig. 4) and f_π is the amplitude for

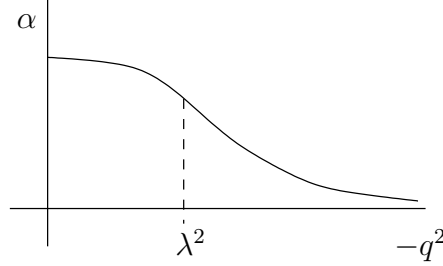


Figure 4:

the pion – axial current transition,

$$\begin{aligned} f_\pi^2 = & \frac{1}{8} \int \frac{d^4 q}{(2\pi)^4 i} \text{Tr} \{i\gamma_5, G^{-1}\} G \{i\gamma_5, G^{-1}\} G A_\mu A_\mu \\ & + \frac{1}{64\pi^2 f_\pi^2} \int \frac{d^4 q}{(2\pi)^4 i} \text{Tr} (\{\gamma_5, G^{-1}\} G)^4. \end{aligned} \quad (2.2)$$

Before turning to the formal solution, let us discuss its general properties and the difference in the structure caused by the inclusion of the pion contribution.

Writing $G^{-1}(q)$ as

$$G^{-1}(q) = Z^{-1}(q) (m(q) - \hat{q}), \quad (2.3)$$

we obtain (2.1) in the form

$$\partial^2 G^{-1} = g(q) \partial_\mu G^{-1} G \partial_\mu G^{-1} + \frac{m^2}{f^2} \frac{m - \hat{q}}{m^2 - q^2} Z^{-1}, \quad (2.4)$$

where $f^2 = \frac{4}{3} \pi^2 f_\pi^2$. For the solution of the equation for G^{-1} without pion contribution (i.e. without the last term in (2.4)) the behaviour of $Z(q^2)$ and $m(q^2)$ as functions of q^2 in the Euclidean region of negative $q^2 = -Q^2$ is shown in Fig. 5.

Here the dashed curve corresponds to the massive quark, $m_0 \neq 0$, and the solid curve to the massless quark, respectively. In the latter case

$$m(q^2) = -\frac{\nu^3}{Q^2}, \quad Q^2 \rightarrow \infty. \quad (2.5)$$

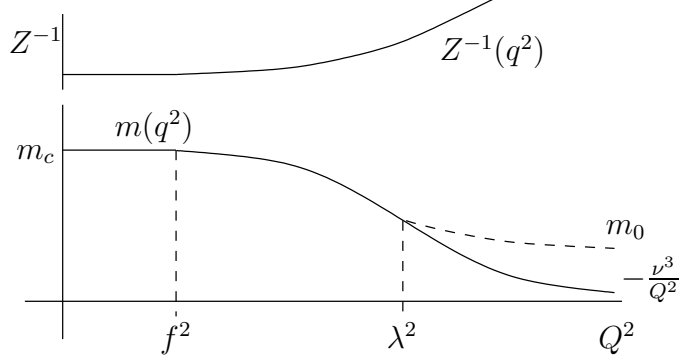


Figure 5:

If we include the last term of (2.4), the solution corresponding to massive quarks disappears, as it was expected. The massless quark solution (2.5) will, however, survive because in this case the last term in (2.4) which can be called Δ_π is small at large Q^2 values:

$$\Delta_\pi = -\frac{\nu^6 \hat{q}}{f^2 Q^6} Z^{-1}, \quad Q^2 \rightarrow \infty. \quad (2.6)$$

Let us see what would be the effect of the pion contribution at small Q^2 . For $Q \ll m_c = m(0)$ (2.4) leads to the following two equations:

$$\partial^2(Z^{-1}m) = \left(\frac{4g}{m_c^2} + \frac{1}{f^2} \right) Z^{-1}m, \quad (2.7)$$

$$\partial^2 Z^{-1} + \frac{2}{q^2} q_\mu \partial_\mu Z^{-1} = \left(\frac{2g}{m_c^2} + \frac{1}{f^2} \right) Z^{-1}. \quad (2.8)$$

We see that the pion produces a hundred percent correction to the effective coupling because $f \sim m_c$ and $g \simeq 0.2$ if we are close to the critical value of g . This change can be crucial. We shall analyse the equation (2.6) more carefully later. For the time being, in order to see what can happen, let us accept (2.7) and (2.8) literally. These simple equations are easy to solve. The solutions are

$$Z^{-1}m = \frac{\mu_1^2}{Q} Z_1(Q/\mu_1), \quad \frac{4g}{m_c^2} + \frac{1}{f^2} = \frac{1}{\mu_1^2}; \quad (2.9)$$

$$Z^{-1} = \frac{\mu_2^2}{Q^2} Z_2(Q/\mu_2), \quad \frac{2g}{m_c^2} + \frac{1}{f^2} = \frac{1}{\mu_2^2}, \quad (2.10)$$

where Z_1 and Z_2 are solutions Z_ν of the Bessel equation with index $\nu = 1, 2$, respectively. The concrete forms of Z_1 and Z_2 depend on the boundary conditions imposed on the solutions. If we want to preserve the behaviour of Z^{-1} and m at small Q^2 values, we have to choose

$$Z_1 \propto J_1(Q/\mu_1), \quad Z_2 \propto J_2(Q/\mu_2), \quad (2.11)$$

with J_1 and J_2 the Bessel functions. In this case, however, the behaviour of Z^{-1} and m will change at large Q^2 values and it is not obvious whether it will be possible to preserve the

asymptotic behaviour (Fig. 5) corresponding to asymptotic freedom. If our aim is to keep the behaviour at large Q^2 unchanged we have to choose Z_1 and Z_2 as superpositions of the singular and non-singular solutions of the Bessel equation,

$$Z_1 = a_1 Y_1(Q/\mu_1) + b_1 J_1(Q/\mu_1), \quad (2.12a)$$

$$Z_2 = a_2 Y_2(Q/\mu_2) + b_2 J_2(Q/\mu_2), \quad (2.12b)$$

and to select $a_{1,2}$ and $b_{1,2}$ such that the asymptotic behaviour at large Q^2 is preserved. For small Q^2 values this means

$$Z_1 \propto \frac{1}{Q}, \quad Z_2 \propto \frac{1}{Q^2} \quad (2.13)$$

and, consequently,

$$Z^{-1} \propto \frac{1}{Q^4}, \quad m \propto Q^2. \quad (2.14)$$

Instead of the behaviour of Z^{-1} and m corresponding to Fig. 5 we now have a behaviour as shown in Fig. 6.

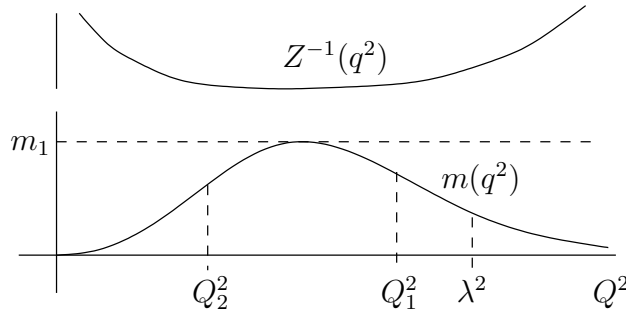


Figure 6:

This behaviour corresponds to the confined solution for the quark Green's function. In this solution the condensate which is created at momenta of the order of λ exists only in a region of Q^2 values between Q_1^2 and Q_2^2 ($Q_1^2, Q_2^2 \sim f^2$) and disappears at smaller Q^2 values due to its decay into π -mesons. Because of the decrease of $m(q^2)$ at large and small Q^2 , in this solution the pion contribution to the right-hand side of the equation (2.4), Δ_π , is localised between Q_1^2 and Q_2^2 (we shall see this in detail later). This localisation of the pion contribution enables us to analyse not only the behaviour in the Euclidean region $q^2 < 0$ but also the analytic properties of the solution and its behaviour at positive q^2 values.

If the pion is localised, $G^{-1}(q)$ satisfies the old equation without Δ_π at $Q^2 \ll Q_1^2$ and $Q^2 \gg Q_2^2$. This means that $G^{-1}(q)$ can be written in the form

$$G^{-1}(q) = C_1(q)G_1^{-1}(q) + C_2(q)G_2^{-1}(q), \quad (2.15)$$

where $G_{1,2}^{-1}(q)$ are two different solutions of the equation (2.4) for $\Delta_\pi = 0$ and $C_{1,2}(q)$ are slowly varying functions,

$$\begin{aligned} C_1(q) &\rightarrow \text{const} \quad \text{at} \quad Q^2 \gg Q_1^2 \quad \text{and} \quad C_1(q) \rightarrow 0 \quad \text{at} \quad Q^2 \ll Q_2^2, \\ C_2(q) &\rightarrow 0 \quad \text{at} \quad Q^2 \gg Q_1^2 \quad \text{and} \quad C_2(q) \rightarrow \text{const} \quad \text{at} \quad Q^2 \ll Q_2^2. \end{aligned}$$

$G^{-1}(q)$ has to satisfy the conditions at large Q^2 which we already imposed on our solution. For this, we are bound to choose $G_1^{-1}(q)$ to be the solution corresponding to symmetry breaking with the "mass" m_c , which was discussed in [6], and $G_2^{-1}(q)$ has to be the solution describing a singular behaviour of the type (2.13), (2.14) at small Q^2 . We have to have in mind also that $G^{-1}(q)$ (2.15) must not have singularities in the complex plane. $G_1^{-1}(q)$ has no singularities there but the standard cut on the real axis from $q^2 = m_1^2$ to $q^2 \rightarrow \infty$. We choose G_2^{-1} to have also no singularities in the complex plane. After that we shall see what will be the singularities of $G^{-1}(q)$.

Making use of the fact that equation (2.4) with $\Delta_\pi = 0$ is scale invariant for $\alpha = \text{const}$, we can always write

$$G_2^{-1}(\hat{q}, g(q)) = \frac{m_2^4}{q^2} \tilde{G}^{-1}\left(\frac{m_2^2}{\hat{q}}, g\left(\frac{m_2^2}{q}\right)\right), \quad (2.16)$$

where $\tilde{G}^{-1}(q)$ satisfies the equation

$$\partial^2 \tilde{G}^{-1}(q) = g\left(\frac{m_2^2}{q}\right) \partial_\mu \tilde{G}^{-1}(q) \tilde{G}(q) \partial_\mu \tilde{G}^{-1}(q). \quad (2.17)$$

This is the same equation which we have discussed in [6]; the behaviour of $\tilde{g}(q) \equiv g(m_2^2/q)$ is $\tilde{g} \rightarrow 0$ at $q \rightarrow 0$ and $\tilde{g}(q) \rightarrow g_0$ at $q \rightarrow \infty$, opposite to that shown in Fig. 4. It was shown in [3] and [6] that independently of the behaviour of g we can always find a solution with a cut along the positive q^2 axis from $q^2 = m_2^2$ to $q^2 \rightarrow \infty$ if we choose the solution not to have singularities at $q = 0$ and if we fix $\tilde{G}^{-1}(q)$ by the condition $\tilde{G}^{-1}(q)|_{q=0} = m_2'$ (m_2 and m_2' are in a simple relation).

Suppose that $\tilde{G}^{-1}(q)$ is chosen in such a way. Then $G_2^{-1}(q)$ defined by (2.16) will have a cut from $q^2 = 0$ to $q^2 = m_2^2$ and a singular behaviour at $q^2 \rightarrow 0$. As a result, $G^{-1}(q)$ has two cuts in the q^2 plane (Fig. 7),

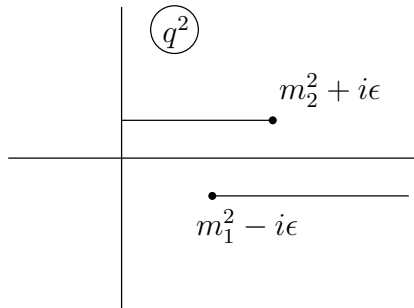


Figure 7:

where we take $m_2 > m_1$ since, as we will see in the next section, this is the only possibility to avoid singularities in the complex plane; due to reasons to be discussed, $i\epsilon$ is positioned in the way shown in Fig. 7.

For the sake of simplicity, let us consider the properties of $G^{-1}(q)$ in the q_0 -plane at the value $\vec{q} = 0$ of the space component of q . We will write $G^{-1}(q)$, as in [6], in the form

$$G^{-1}(q_0) = G_+^{-1}(q_0) \frac{1 + \gamma_0}{2} + G_-^{-1}(q_0) \frac{1 - \gamma_0}{2}. \quad (2.18)$$

For example, $G_+^{-1}(q_0)$ has two normal cuts (Fig. 8).

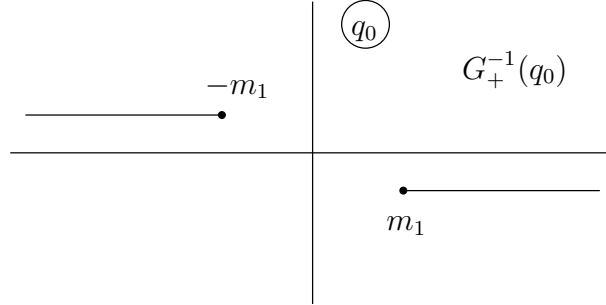


Figure 8:

The singularities of $G_{1+}^{-1}(q_0)$ at $q_0 = m_1$ and $q_0 = -m_1$ are different. It is clear from eq. (103) in [6] that $G_{1+}^{-1}(q_0 = m_1) = 0$, while $G_{1-}^{-1}(q_0 = m_1)$, for $g < \frac{1}{2}$, is different from zero: $G_{1-}^{-1}(q_0 = m_1) = G_{1+}^{-1}(q_0 = -m_1) = \text{const.}$

The function $\tilde{G}_+^{-1}(q_0)$ also has the analytic structure of Fig. 8 with $m_1 \rightarrow m_2$. In the course of the reflection $q_0 \rightarrow -m_2^2/q_0'$ the points on the line $q_0 = iQ$ transform into $q_0' = im_2^2/Q$; the points $q_0 = \pm m_2 \mp i\varepsilon$ transform into $q_0' = \mp m_2 \mp i\varepsilon$, respectively. As it follows from all this, G_+^{-1} has singularities corresponding to Fig. 9.

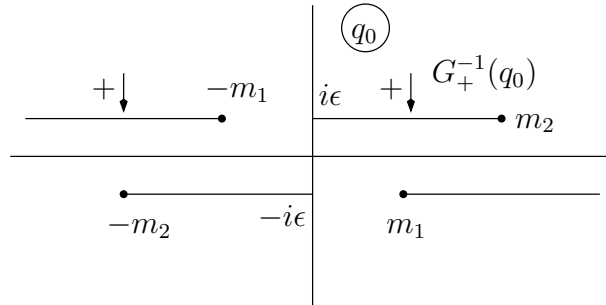


Figure 9:

These analytic properties are a clear manifestation of the fact that the Dirac sea is destroyed; G_+^{-1} has singularities corresponding to both positive and negative energies. The parameter m_2 has the meaning of the Fermi energy. In order to find zeros of G_+^{-1} which have to be in the lower q_0 half plane and correspond to unstable quarks with positive and negative energy, we have to know the signs of $\text{Im } G_{1+}^{-1}$, $\text{Im } G_{2+}^{-1}$ and the signs of C_1 , C_2 in (2.15). The solutions $G_{1+}^{-1}(q_0)$ and $\tilde{G}_+^{-1}(q_0)$ satisfy the normal unitarity condition. Their imaginary parts

at positive q_0 have to be negative. This leads to signs of the imaginary parts as shown in Fig. 9 (with arrows pointing at the positive side of the cuts). Having this in mind, we can write $G_1^{-1}(\hat{q})$ near to its zero (i.e. at q_0 close to m_1) in the form

$$G_{1+}^{-1} = (m_1 - i\delta - q_0)^{\frac{1}{\beta}} \quad , \quad \frac{1}{2} < \beta < 1 . \quad (2.19)$$

Since G_{2+}^{-1} remains finite at $q_0 \rightarrow m_1$, it can be given in the form

$$G_{2+}^{-1}(q_0) = \rho e^{-i\phi} \quad , \quad 0 < \phi < \pi . \quad (2.20)$$

If so,

$$G_+^{-1}(q_0) = C_1(m_1 - i\delta - q_0)^{\frac{1}{\beta}} + C_2\rho e^{-i\phi} . \quad (2.21)$$

The zeros of $G_+^{-1}(q_0)$ are then defined by the equation

$$q_0^* = m_1 - i\delta + \left(\frac{\rho C_2}{C_1} \right)^{\beta} e^{-i[\beta\phi + (1-\beta)\pi]} . \quad (2.22)$$

If $\frac{C_2}{C_1} > 0$, we have $\text{Im } q_0^* < 0$. In this case the singularity appears in the lower half plane and describes the unstable positive energy quark. Repeating the calculation for $q_0 \rightarrow -m_2$, we obtain a singularity corresponding to the unstable hole. Considering $G_-^{-1}(q_0)$ instead of $G_+^{-1}(q_0)$, we find the same singularities for an anti-quark and an anti-hole.

If the condition $\frac{C_2}{C_1} > 0$ is not satisfied the singularities can move to the upper half plane. This does not destroy the theory because they will be on the unphysical sheet. However, in this case I do not have any simple interpretations for these singularities.

The analytic properties of $G_+^{-1}(q)$ presented in Fig. 9 imply that in the limit $\varepsilon \rightarrow 0$ the Feynman Green's function defined for real q_0 values becomes a non-analytic function. Two analytic functions which have no singularities in the upper and lower complex half planes can be defined and called the retarded and the advanced Green's function. At finite $i\varepsilon$ there exists one analytic function with four cuts. This can be easily seen if we consider $G_+^{-1}(q)$ as a function of q_0 at a fixed value of the space component \vec{q} of the 4-vector q_μ . In this case we will have Fig. 10 instead of Fig. 9.

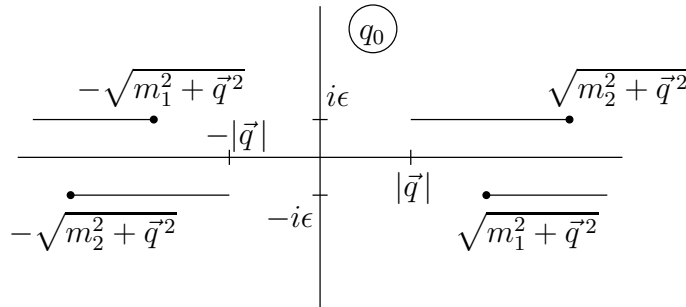


Figure 10:

When negative energies are involved, it is natural to expect that for the exact solution all four cuts have discontinuities different from zero in the intervals from $q_0 = |\vec{q}|$ to $q_0 \rightarrow \infty$ and from $q_0 \rightarrow -\infty$ to $q_0 = -|\vec{q}|$.

If in the usual, non-confined case we know the Green's function (calculating it by using Feynman diagrams in the Euclidean space), we can continue it into positive q^2 values and find that the discontinuity at $q^2 > m^2$ satisfies the unitarity condition. This means that the retarded Green's function coincides with the Feynman Green's function.

The confined case is more complicated. The knowledge of the retarded Green's function in the limit ($i\varepsilon \rightarrow 0$) is not sufficient for finding the Feynman Green's function. In order to obtain the Feynman Green's function, we need the equation for the discontinuities on the new cuts; it will be an equation for the density matrix of quarks in the vacuum.

In the next section we will find the solution of the equation (2.1) in the limit $i\varepsilon \rightarrow 0$ (retarded Green's function) without poles and with the properties we have discussed. In section 4 we shall obtain the equations for the discontinuities on the new and old cuts.

3 Solution for the retarded Green's function of confined massless quarks

In this section I follow the pattern formulated in the previous section. I will find the solution of the equation (2.1) in Euclidean space and then, to be sure that it is stable, continue it into the complex plane. To find the confined solution of the equation (2.1) for the Green's function of light quarks, we will introduce the same representation for G^{-1} as in [6]:

$$G^{-1}(q) = \left(\frac{u}{q}\right)^{\frac{1}{\beta}} e^{-\hat{n}\frac{\phi}{2}} \quad (3.1)$$

where $\beta = 1 - g$ and $\hat{n} = \hat{q}/q$. Instead of the equations (84), (85) in [6], we will have

$$\ddot{\phi} + \frac{2\dot{u}}{u}\dot{\phi} - 3\sinh\phi = 0, \quad (3.2a)$$

$$\ddot{u} - u + \left[\beta^2 \left(3\sinh^2\frac{\phi}{2} + \frac{\dot{\phi}^2}{4} \right) - \frac{q^2\beta\cosh^2\frac{\phi}{2}}{f^2} \right] u = \frac{\dot{\beta}}{\beta}(\dot{u} - u), \quad (3.2b)$$

where $\dot{f} = \frac{\partial f}{\partial \xi}$ and $\xi = \ln q$. As we see, the pion contribution to the equation (2.1) influences only the equation for $u(\xi)$ and it depends explicitly on q^2 . Because of this, for the equations (3.2) the energy is not conserved even if β is constant. In the Euclidean region, $q^2 = -Q^2 < 0$, we can write $\phi = i\psi$ and the equations take the form

$$\ddot{\psi} + 2p\dot{\psi} - 3\sin\psi = 0, \quad (3.3a)$$

$$\ddot{u} - V(\xi)u = 0, \quad (3.3b)$$

where

$$V(\xi) = 1 + \beta^2 \left(3 \sin^2 \frac{\psi}{2} + \frac{\dot{\psi}^2}{4} \right) - \frac{Q^2}{f^2} \beta \cos^2 \frac{\psi}{2} + \frac{\dot{\beta}}{\beta} (p - 1) \quad (3.4)$$

and $p = \dot{u}/u$. As before, the equation (3.3a) corresponds to particle propagation in a periodic potential with damping when ξ is increasing and with acceleration when ξ is decreasing.

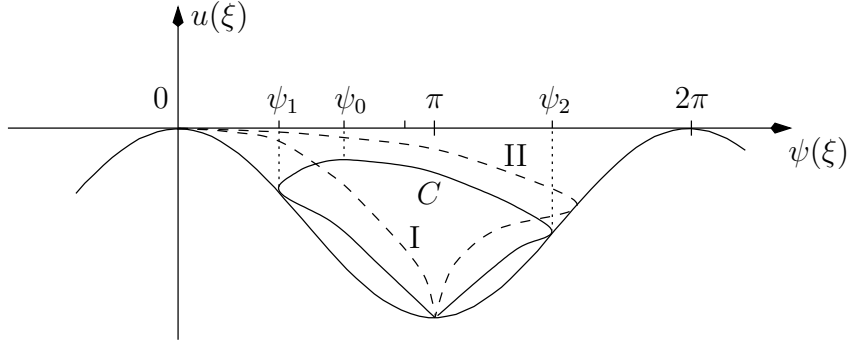


Figure 11:

In [6] we considered the trajectories of the type I and II (dashed curves); now we will concentrate mainly on the trajectory C (solid curve) which has the structure we discussed in the previous section. Any given trajectory defines the potential $V(\xi)$ (if we neglect $\frac{\dot{\beta}}{\beta}(\dot{u} - u)$) in the equation (3.3b) which is the Schrödinger equation at zero energy. The solution of this equation, defining the damping p in (3.3a), has to be chosen self-consistently.

The structure of the equations (3.3) with pion contribution differs essentially from the structure of the equations without pions even at large Q^2 in the sense that they have no solutions corresponding to massive quarks. The massless solutions of these equations are not very different with or without π -mesons.

The solutions of (3.3) satisfying the condition of asymptotic freedom are, at large Q^2 ,

$$\frac{1}{2}(\psi - \pi) = \frac{\nu^3}{Q^2} \left(\frac{\alpha}{\alpha_0} \right)^{-3\gamma}, \quad (3.5a)$$

$$u = Q^2 u_0 \left\{ \left(\frac{\alpha}{\alpha_0} \right)^\gamma + \frac{\nu_1^4}{Q^4} \left(\frac{\alpha}{\alpha_0} \right)^{-\gamma} - \frac{\nu^6}{8f^2 Q^4} \frac{\pi}{2} \left(\frac{\alpha}{\alpha_0} \right)^{-2\gamma} \right\}, \quad (3.5b)$$

where $\gamma = \frac{4}{b}$ is the invariant anomalous dimension; $b = \frac{11}{3}N_c - \frac{2}{3}n_f$. The renormalisation of the Green's function which we discussed in the previous section is

$$Z^{-1}(Q) = u_0 \left(\frac{\alpha}{\alpha_0} \right)^{\gamma/\beta} \quad \text{at} \quad Q \rightarrow \infty \quad (3.6)$$

in Feynman gauge (which we are using here).

It is not clear at all whether it makes sense to take these anomalous dimensions seriously. For the sake of simplicity, we shall consider (3.5) at $\gamma = 0$. Important is, that the solutions of (3.3) still contain two parameters.

For small Q^2 values the non-confined solutions can be written in the simple form

$$\psi = \frac{Q}{m_c}, \quad (3.7a)$$

$$u = Q \left\{ 1 + \frac{1}{8} \beta(0) \left(\beta(0) \frac{Q^2}{m_c^2} - \frac{Q^2}{f^2} \right) \right\}. \quad (3.7b)$$

The confined solution has a more complicated structure. For $Q^2 \rightarrow 0$, $\psi \rightarrow \pi$ we have in this case

$$\frac{\psi - \pi}{2} \simeq \left(\frac{Q}{m_2} \right)^p C \cos \left(\sqrt{2 - 3\beta^2} \ln \frac{Q}{Q_0} \right), \quad (3.8a)$$

$$u \simeq \left(\frac{m_2}{Q} \right)^p u_0 \left\{ 1 - \left(\frac{Q}{m_2} \right)^{2p} \frac{\beta^2 C^2}{p} \ln \frac{Q}{Q_1} + \left(\frac{Q}{m_2} \right)^{2p} \frac{\beta^2 C^2}{\sqrt{2 - 3\beta^2}} \cos \left(2\sqrt{2 - 3\beta^2} \ln \frac{Q}{Q_0} + \delta \right) \right\}, \quad (3.8b)$$

with $p = \sqrt{1 + 3\beta^2}$, $\beta = \beta(0)$.

The solutions contain three essential parameters C , Q_0 and Q_1 which define $\tilde{\psi} = \psi - \pi$, $\dot{\tilde{\psi}}$ and \dot{u} at $Q = m_2$; $C = \tilde{\psi}_0/2$,

$$\frac{\dot{\tilde{\psi}}_0}{2} = p - \sqrt{2 - 3\beta^2} \tan \left(\sqrt{2 - 3\beta^2} \ln \frac{m_2}{Q_1} \right). \quad (3.9)$$

Let us now consider the structure of the solution in the intermediate region. We will start with the qualitative discussion of the non-confined solution of the type I. In this case the potential $V_0(\xi)$ in (3.3b) without pion contribution behaves as shown in Fig. 12 (solid line) and the solution $u_0(\xi)$ corresponds to the dashed curve in the same figure, where λ is the QCD scale at which $\beta^2 = 2/3$ and m_c is the quark mass.

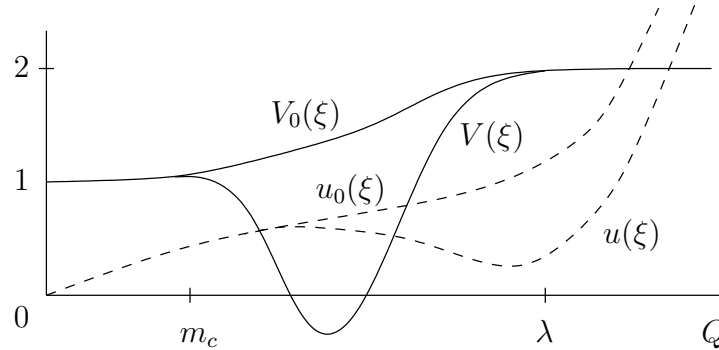


Figure 12:

The pion-induced potential

$$V_\pi(\xi) = -\frac{Q^2}{f^2}\beta \cos^2 \frac{\psi}{2} \quad (3.10)$$

decreases at large and small Q^2 values:

$$V_\pi = -\frac{Q^2}{f^2}\beta(0) \quad \text{at} \quad Q^2 < m_c^2, \quad V_\pi = -\frac{\nu^6}{f^2 Q^4} \quad \text{at} \quad Q^2 > \lambda^2.$$

If $f \sim m \sim \nu < \lambda$, as it is natural to expect from the expression for V_π , the total potential V becomes essentially different from $V_0(\xi)$, especially for small $\beta(0)$ values. It will correspond roughly to the second solid curve in Fig. 12. The solution $u(\xi)$ of the equation (3.3b) also changes substantially. Its exact form depends, of course, on the values of f , ν and on the behaviour of $\beta(0)$. At sufficiently small $\beta(0)$ it can even have a shape $u(\xi)$ corresponding to the second dashed line in Fig. 12. From the point of view of the structure of the solution in Euclidean space, these changes do not matter too much (at least at the first sight). But, as we will see, from the point of view of the analytic continuation the situation is different.

Let us consider now the behaviour of the potential $V(\xi)$ and the solution $u(\xi)$ corresponding to the "confined" trajectory C . In this case $V_0(\xi)$ and $u_0(\xi)$ behave as shown in Fig. 13.

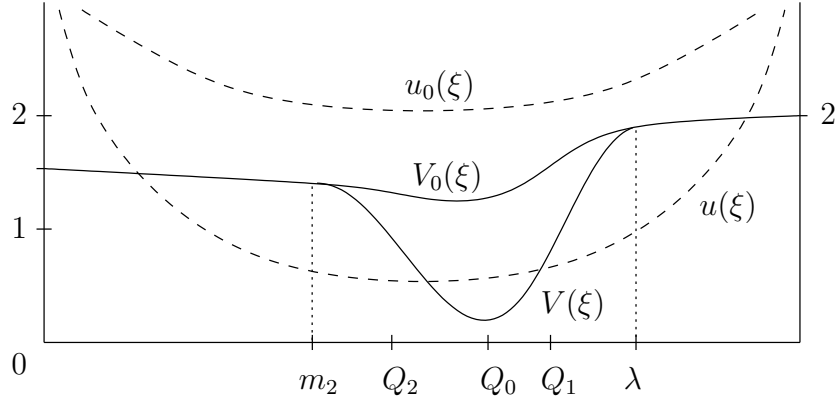


Figure 13:

The pion potential $V_\pi(\xi)$ in this case is

$$V_\pi(\xi) = \begin{cases} -\frac{\nu^6}{f^2 Q^4} & \text{at } Q > \lambda \\ -\beta \frac{Q^2}{f^2} \left(\frac{Q}{m_2}\right)^{2\beta} \frac{1}{2} \left[1 + \cos \left(2\sqrt{2-3\beta^2} \ln \frac{Q}{Q_0} \right) \right] & \text{at } Q < m_2. \end{cases} \quad (3.11)$$

This potential is strongly localised near the value $Q=Q_0$ where the trajectory C reaches its highest point (point ψ_0 in Fig. 11). If this highest point is in the region close to zero, the minimum of $V_\pi(\xi)$ equals $-Q_0^2\beta(Q_0)/f^2$. As a result, the potential $V(\xi)$ has a behaviour shown in Fig. 13. The solution $u(\xi)$ looks qualitatively the same. At some point its derivative $\dot{u}(\xi)$ changes sign, which leads to the transition from acceleration to damping in the equation

(3.3a). As a result, the trajectory returns to the minimum of the well. Obviously, there is always a solution for $u(\xi)$ with such a behaviour. Because of this, a solution of the type C for $\psi(\xi)$ also exists and depends on two parameters ν_1 and Q_0 . The problem with this solution is not its existence in Euclidean space but its behaviour at complex q^2 .

In order to understand the problem of the analytic continuation, we have to remember that the singularity of G^{-1} corresponds to the point where

$$u(q) = 0$$

and find out how the position of this zero depends on the structure of $u(\xi)$ at negative q^2 .

Let us start with the simple quasi-classical solution for u :

$$u = u_0 \cosh \zeta(\xi) \quad , \quad \zeta(\xi) = \int_{\xi_0}^{\xi} \sqrt{V(\xi')} d\xi' , \quad (3.12)$$

where ξ_0 is chosen so that $\dot{u}(\xi_0) = 0$, and consider the analytic continuation of (3.12) along the circle in the complex plane of $q = Q_0 e^{i(\frac{\pi}{2} - \chi)}$, $\chi \geq 0$; $\xi_0 = \ln Q_0$ (see Fig. 14).

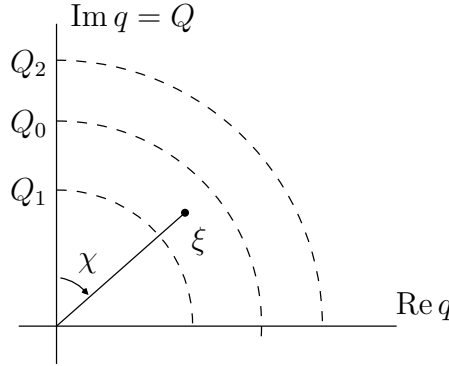


Figure 14:

In this continuation we have

$$\begin{aligned} \zeta(\xi) &= -i \int_0^{\chi} \sqrt{V\left(\xi_0 + \frac{i\pi}{2} - i\chi'\right)} d\chi' = \zeta_1 - i\zeta_2 , \\ u &= \cosh \zeta_1 \cos \zeta_2 - i \sinh \zeta_1 \sin \zeta_2 ; \end{aligned} \quad (3.13)$$

u will have a zero at the point $\zeta_2 = \frac{\pi}{2}$, $\zeta_1 = 0$. The condition $\zeta_1 = 0$ means that the singularity appears near the circle where $\dot{u}(\xi_0) = 0$. The condition $\zeta_2 = \frac{\pi}{2}$ gives

$$\zeta_2 = \chi \sqrt{V(\xi_0)} , \quad \chi = \frac{\pi}{2\sqrt{V(\xi_0)}} . \quad (3.14)$$

Hence, we will have a singularity in the *upper* half-plane if $V(\xi_0) > 1$, and in the *lower* half-plane, on the unphysical sheet, if $V(\xi_0) < 1$.

From (3.4) it is obvious that if the pion potential is not present, then $V(\xi) > 1$ and there will be a singularity on the physical sheet if the solution has a minimum (the acceleration transforms into damping). But with the pion potential included, $V(\xi_0)$ can be less than unity, and the singularity will be on the unphysical sheet if we choose a solution with a minimum close to the minimum of the potential. At the same time, considering the behaviour of the solution for the non-confined trajectory (Fig. 12), we see the opposite situation: without the pion potential $u_0(\xi)$ has no zeros and thus there is no reason for singularities. However, if in the presence of the pion potential at a small $\beta(0)$ the solution $u(\xi)$ shown in Fig. 12 exists and has a minimum in the region where $V(\xi) > 1$, we will definitely have a singularity in the upper half plane. It is important to stress that for the non-confined trajectory the position of the minimum is defined by the form of the potential and by the condition according to which the solution has to approach zero in the limit $Q \rightarrow 0$. This means that at least for $g(0)$ close to unity the non-confined solution will be unstable.

We shall use this qualitative considerations as a hint how to obtain constructively the stable solution for the confined trajectory. Let us consider the trajectory C for which ψ_0 , defined as the point where $\dot{u}(\xi_0) = 0$, is very small, $\psi \ll 1$, and so is ψ_1 where $\dot{\psi} = 0$. In this case the potential $V(\xi)$ in (3.3b) will be determined mainly by the pion potential. In addition, it follows from (3.3a) that $\psi(\xi)$ will be a slowly changing function of ξ near ξ_0 where $\dot{\psi} = 0$ and $\dot{u} = 0$. In this region the equation (3.3b) can be written as

$$\ddot{u} - \nu^2 u + x^2 \mu^2 u = 0 \quad (3.15)$$

where $\nu^2 = 1 + \beta^2 \left(3 \sin^2 \frac{\psi}{2} + \frac{\dot{\psi}^2}{4} \right)$, $\mu^2 = \beta^{-1} \cos^2 \frac{\psi}{2}$ and $x = \frac{Q}{f} \beta$ with slowly varying ν and μ , $\nu^2 \approx 1$ and $\mu^2 \approx \beta^{-1}$.

For constant μ and ν values, (3.15) is the Bessel equation in $x \simeq \ln \xi$. Its solution can be given in the form

$$u = c_1 Y_\nu(\mu x) + c_2 J_\nu(\mu x). \quad (3.16)$$

We choose the coefficients c_1, c_2 in such a way that $\dot{u}(\xi_0) = 0$ at a point $x_0 = Q_0 f / \beta(x_0)$ inside the region between Q_1 and Q_2 where ν is close to unity.

Outside this region $\dot{u}(\xi) \neq 0$. Indeed, in the $x \rightarrow 0$ limit only the singular Bessel function is important,

$$u = c_1 Y_\nu(\mu x) \sim (\mu x)^{-\nu}. \quad (3.17)$$

For large x , as it can be seen from (3.11), u also has a power behaviour (3.17) (only with different $\mu(Q)$ and $\nu(Q)$).

Thus we conclude that in the dangerous region where $\dot{u}(\xi)$ can be zero we have an explicit expression for

$$u(\xi) = c_1 Y_1(x) + c_2 J_1(x), \quad (3.18)$$

which allows us to carry out the analytic continuation along the strip shown in Fig. 14 and to see where the zeros of $u(\xi)$ are.

The most interesting case is when the singularity appears near the real axis in the q plane: $\chi = \frac{\pi}{2} + \delta$,

$$\begin{aligned} J_1(e^{-i\frac{\pi}{2}}x') &= -iI_1(x') , \\ Y_1(e^{-i\frac{\pi}{2}}x') &= -\frac{2}{\pi}iK_1(x') - I_1(x') . \end{aligned} \quad (3.19)$$

The equation for the position of the singularity is

$$-i \left[\frac{2}{\pi}K_1(x') - \gamma I_1(x') \right] - I_1(x') = 0 , \quad \gamma = -\frac{c_2}{c_1} = \frac{\dot{Y}_1(x_0)}{\dot{J}_1(x_0)} . \quad (3.20)$$

It is clear from this equation that there is no singularity on the real axis. Near the real axis, $x' = xe^{-i\delta} \approx x - i\delta x$, we have

$$\begin{aligned} \frac{2}{\pi}K_1(x) - \gamma I_1(x) - \dot{I}_1(x) \cdot \delta &= 0 , \\ \left(\frac{2}{\pi}\dot{K}_1(x) - \gamma \dot{I}_1(x) \right) \cdot \delta + I_1(x) &= 0 , \quad \dot{f} = x\partial_x f(x) . \end{aligned} \quad (3.21)$$

If x is not small, there is no reason to expect a singularity near the real axis since in this case the potential in (3.15) is much less than unity. For small x values we have

$$\frac{2}{\pi}K_1(x) \simeq \frac{2}{\pi x} \left(1 + \frac{x^2}{2} \ln \frac{x}{c} \right) ; \quad I_1(x) \simeq \frac{x}{2} . \quad (3.22)$$

The γ parameter for $x_0 \ll 1$ becomes

$$\gamma \equiv \frac{\dot{Y}_1(x_0)}{\dot{J}_1(x_0)} = \frac{4}{\pi x_0^2} \gg 1 , \quad (\gamma > 1 \quad \text{for} \quad x_0 < 3) . \quad (3.23)$$

Using (3.22) it is easy to derive the solution of (3.21):

$$\delta \simeq \frac{1}{2\gamma} , \quad x^2 \simeq \frac{4}{\pi\gamma} \approx x_0^2 . \quad (3.24)$$

Hence, the singularity is on the unphysical sheet ($\delta > 0$). It is positioned on the dangerous circle $x = x_0$ and near the real axis when x_0 is small.

Performing the analytic continuation we supposed that ψ is changing slowly as the function of q . This hypothesis is correct, if the singularity is far away from the real axis ($\delta > 1$). If, however, $\delta \ll 1$, we have to be careful: near the singularity the trajectory $\phi(\xi)$ changes fast, jumping to a large value $\phi \sim \ln 1/\delta$.

Fortunately, this jump does not influence essentially the behaviour of $u(\xi)$ or the position of the singularity. At first sight this jump is important because near the singularity we have

$$u \sim \sqrt{\mu^2 - q^2} , \quad \phi \sim \frac{1}{\mu^2 - q^2} , \quad (3.25)$$

and in the equation for u two terms \ddot{u} and $u\dot{\phi}^2/4$ are of the same order. Let us, however, consider the equation for $z = u^2$. We can write this equation in the form

$$\ddot{z} - 2 \left(1 - 3\beta^2 \sinh^2 \frac{\phi}{2} + \frac{q^2}{2f^2} \beta \cosh^2 \frac{\phi}{2} \right) z - \frac{1}{2} \left(\frac{\dot{z}^2}{z^2} - \beta^2 \dot{\phi}^2 \right) z = 0. \quad (3.26)$$

It is easy to show that the last term in this equation has a finite limit E when $q^2 \rightarrow \mu^2$. Hence, the equation can be rewritten as

$$\ddot{z} - 2 \left(1 - 3\beta^2 \sinh^2 \frac{\phi}{2} + \frac{q^2}{2f^2} \beta \cosh^2 \frac{\phi}{2} \right) z + E = 0. \quad (3.27)$$

Its solution near the singularity is

$$z = (q^2 - \mu^2) + c(q^2 - \mu^2)^{3-\frac{1}{\beta}} \quad ; \quad e^\phi \sim (\mu^2 - q^2)^{-1/\beta} \quad (3.28)$$

and the correction to $z = u^2$ from the jump in the trajectory turns out to be small if $\beta > \frac{1}{2}$.

4 Analytic properties of the Green's functions of confined quarks

In the previous sections we have shown that the equations for Green's functions are not sufficient to define the theory. It is easy to show that without confinement the requirement of usual analytic properties for the Green's functions is enough for defining the solution for the Green's functions. But even in this case it is not clear a priori, what kind of bound states have to be introduced and how these states would influence the equations for Green's functions. In particular, we have to see how Goldstone type states which necessarily have to exist in some cases will affect the equations. This question will be discussed later. Having it in mind, we first have to learn what kind of analytic properties are necessary for the Green's functions of quarks and gluons if there is confinement.

Let us start with the usual definition (given by Dyson) for the Green's function of the quark:

$$\begin{aligned} G_D(x - x') &= \langle T \Psi(x) \bar{\Psi}(x') \rangle \\ &= \vartheta(x_0 - x'_0) \langle \Psi(x) \bar{\Psi}(x') \rangle - \vartheta(x'_0 - x_0) \langle \bar{\Psi}(x') \Psi(x) \rangle. \end{aligned} \quad (4.1)$$

The quantity on the right-hand side can be written in the form

$$\langle \Psi(x) \bar{\Psi}(x') \rangle = \int \frac{d^4 p}{(2\pi)^4} f(p) e^{-ip(x-x')}, \quad (4.2)$$

where

$$\overline{f(p)} = \gamma_0 f^+(p) \gamma_0 = f(p), \quad (4.3)$$

$$f^+(p) = \sum_n \langle 0 | \Psi(0) | n \rangle \langle n | \bar{\Psi}(0) | 0 \rangle \delta(p - p_n) , \quad (4.4)$$

and

$$\langle \bar{\Psi}(x') \Psi(x) \rangle = \int \frac{d^4 p}{(2\pi)^4} \tilde{f}(p) e^{-ip(x-x')} ; \quad (4.5)$$

$$\bar{\tilde{f}}(p) = \tilde{f}(p) , \quad (4.6)$$

$$\tilde{f}(p) = \sum_n \langle 0 | \bar{\Psi}(0) | n \rangle \langle n | \Psi(0) | 0 \rangle \delta(p + p_n) . \quad (4.7)$$

Making use of charge conjugation, we can see that

$$\tilde{f}(p) = C^{-1} f(-p) C . \quad (4.8)$$

The usual hypothesis which leads to simple analytic properties for $G(p)$ is

$$p_n^2 \geq 0 , \quad p_{n0} > 0 , \quad (4.9)$$

for the energy-momentum of the intermediate states p_n in (4.2) and (4.5). If this were true the quarks would be observable.

If there are no stationary states with quark quantum numbers, the functions $f(p)$ and $\tilde{f}(p)$ are still related by (4.8) and they still satisfy (4.3) and (4.6) but no other simple properties. It can be said only that the Dyson T -product G_D can be written in momentum space as the sum of two analytic functions G_1, G_2 :

$$G_D = G_1 - G_2 , \quad (4.10a)$$

$$G_1(p_0, \vec{p}) = \frac{1}{\pi} \int_{-\infty}^{\infty} \frac{dp'_0}{p'_0 - p_0 - i\varepsilon} f(p'_0, \vec{p}) , \quad (4.10b)$$

$$G_2(p_0, \vec{p}) = \frac{1}{\pi} \int_{-\infty}^{\infty} \frac{dp'_0}{p'_0 - p_0 + i\varepsilon} \tilde{f}(p'_0, \vec{p}) \quad (4.10c)$$

Nevertheless, we will see that the requirements of causality and unitarity impose severe restrictions on the functions $f(p)$ and $\tilde{f}(p)$.

Let us regard first the causality. In order to exploit it, consider the retarded Green's function

$$G_R(x - x') = \vartheta(x_0 - x'_0) \{ \Psi(x), \bar{\Psi}(x') \} . \quad (4.11)$$

In momentum space G_R can be written in terms of the same functions $f(p)$ and $\tilde{f}(p)$

$$G_R(p_0, \vec{p}) = G_1(p_0, \vec{p}) + G_2^*(p_0, \vec{p}) , \quad (4.12)$$

where

$$G_2^*(p_0, \vec{p}) = \frac{1}{\pi} \int_{-\infty}^{\infty} \frac{dp'_0}{p'_0 - p_0 - i\varepsilon} \tilde{f}(p'_0, \vec{p}) . \quad (4.13)$$

The Green's function (4.11) has to be zero for $(x-x')^2 < 0$. This condition can be formulated in terms of $f(p)$ and $\tilde{f}(p)$ as

$$f(p) = -\tilde{f}(p) \quad \text{at} \quad p^2 < 0. \quad (4.14)$$

The results (4.10) and (4.12)-(4.14) can be expressed in terms of one analytic function in the complex plane with cuts as shown in Fig. 15.

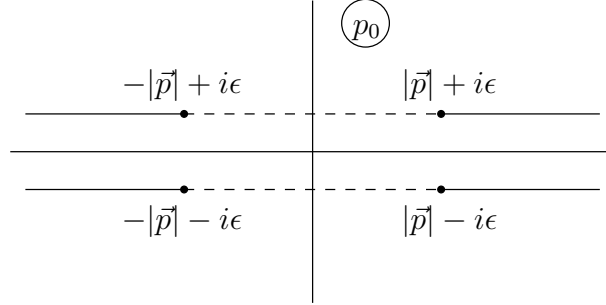


Figure 15:

The Dyson Green's function is defined for real p_0 values and has an imaginary part different from zero everywhere. The retarded Green's function is defined in the upper half plane and, due to the condition (4.14), has no imaginary part between $-|\vec{p}|$ and $|\vec{p}|$. This means that G_R can be defined in the complex plane with four cuts (Fig. 16) provided $i\varepsilon$ is finite.

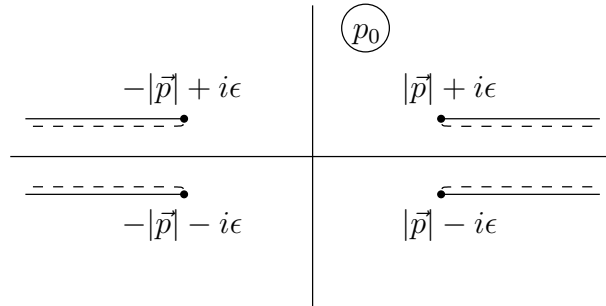


Figure 16:

In order to find the analytic properties corresponding to Fig. 16, the cuts denoted by the dashed lines have been moved from the region $-|\vec{p}| < p_0 < |\vec{p}|$ to the regions $p_0 > |\vec{p}|$ and $p_0 < -|\vec{p}|$. Of course, this procedure defines a new function, different from G_D , on the real axis; it is natural to call it the Feynman Green's function G_F . It is, I believe, possible to show that this function corresponds to the Fourier component of

$$G_F(x, x') = \langle TS\Psi(x)\bar{\Psi}(x') \rangle \quad (4.15)$$

where S is the S -matrix in interaction representation; $|\rangle, \langle|$ are free vacuum states. $G_F(x-x')$ is usually calculated as a series of Feynman diagrams. Generally speaking, (4.1) is not equal to (4.15).

Independently of introducing G_F , Fig. 16 suggests that we can define two functions G_+ , G_- . $G_+(p)$ is the contribution of the usual cuts $(|\vec{p}| - i\varepsilon, \infty)$, $(-\infty, -|\vec{p}| + i\varepsilon)$

$$\begin{aligned} G_+(p) &= \frac{1}{\pi} \int_{|\vec{p}| - i\varepsilon}^{\infty} \frac{dp'_0 \Delta_+(p_0, \vec{p})}{p'_0 - p_0} - \frac{1}{\pi} \int_{-\infty}^{-|\vec{p}| + i\varepsilon} \frac{dp'_0 \Delta_+(-p_0, \vec{p})}{p'_0 - p_0} \\ &= \frac{1}{\pi} \int_{0 - i\varepsilon}^{\infty} \frac{dp'^2}{p'^2 - p^2} \Delta_+(p'^2) \end{aligned} \quad (4.16)$$

and $G_-(p)$ is the contribution of the new cuts

$$G_-(p) = \frac{1}{\pi} \int_{0 + i\varepsilon}^{\infty} \frac{dp'^2}{p'^2 - p^2} \Delta_-(p'^2). \quad (4.17)$$

The expressions (4.16) and (4.17) have to be understood in the usual way, as equations for two invariant functions. The discontinuities Δ_+ and Δ_- are now complex but $\Delta_+ + \Delta_-$ is real. The unitarity relations which under the usual (non-confined) circumstances define the discontinuities on the normal cuts have to define also the new discontinuities. To find them is equivalent to finding the functions $f(p)$ and $\tilde{f}(p)$ which are the imaginary parts of the Dyson Green's function and the retarded Green's function, respectively:

$$\text{Im } G_D(p) = f(p) - \tilde{f}(p), \quad (4.18a)$$

$$\text{Im } G_R(p) = f(p) + \tilde{f}(p). \quad (4.18b)$$

5 Unitarity relations for quark and gluon Green's functions

Let us try to calculate $\langle \Psi(x) \bar{\Psi}(x') \rangle$ using the hypothesis that the interaction can be introduced adiabatically in the theory. This idea is not obvious at all. In the normal perturbative case it means that starting with a free theory and introducing the interaction adiabatically, we gradually reach the vacuum state corresponding to a theory which includes interaction (curve *a* in Fig. 17).

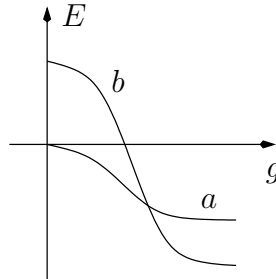


Figure 17:

But if the spectrum of the theory with interaction differs drastically from the spectrum of the free theory, this hypothesis will not work because there has to be level crossing. The

curve which has a chance to reach the physical vacuum (curve b in Fig. 17) starts not at a vacuum state with $g = 0$ but at an excited state. In our case the adiabatic hypothesis is equivalent to the assumption that there exist some excited states in the free theory from which the physical vacuum can be reached by introducing the interaction adiabatically.

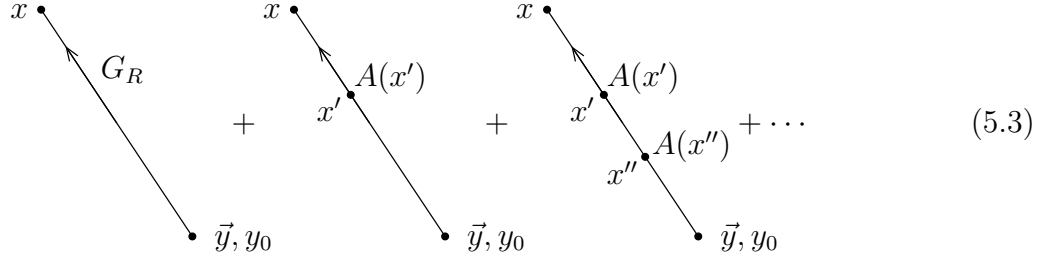
In order to calculate $\langle \Psi(x) \bar{\Psi}(x') \rangle$, let us consider the Dirac equation for the quark field $\Psi(x)$

$$(\hat{\partial} - \hat{A})\Psi - m\Psi = 0; \quad (5.1)$$

here \hat{A} is the operator of the potential for the colour field. The operator Ψ can be written in terms of its initial conditions at $t \rightarrow -\infty$ in the form

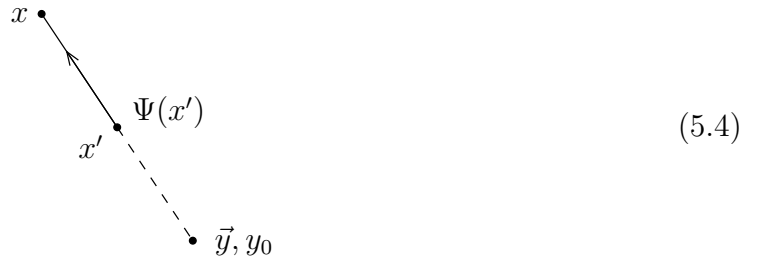
$$\begin{aligned} \Psi(x) = & \int_{y_0 \rightarrow -\infty} d^3y \left[\partial_0 G_R^0(x-y) \Psi(y) + G_R^0(x-y) \partial_0 \Psi(y) \right] \\ & + \int d^4x' G_R^0(x-x') \hat{A} \Psi(x'), \end{aligned} \quad (5.2)$$

where G_R is the retarded Green's function of the free Dirac equation. Diagrammatically (5.2) can be expressed in the form



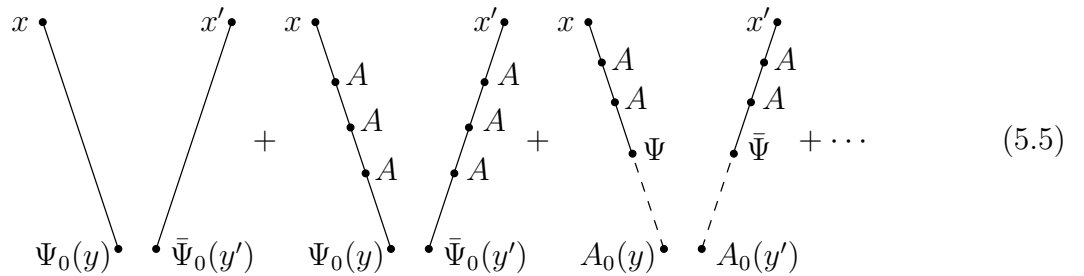
$$(5.3)$$

Expressing A through its initial conditions we will have, for example, the diagram



$$(5.4)$$

instead of the second diagram in (5.3); the dashed line corresponds to the solution of the free equation for the gluonic potential. Doing now the same for $\bar{\Psi}(x')$ with the advanced Green's function, we obtain for $\Psi(x) \bar{\Psi}(x')$ the following diagrammatic structure, where $y_0 = y'_0$:



$$(5.5)$$

Let us denote

$$\begin{aligned}\langle \Psi(x) \bar{\Psi}(x') \rangle &= \text{---} \leftarrow \times \text{---} \\ \langle A(x) A(x') \rangle &= \text{---} \times \text{---} .\end{aligned}\quad (5.6)$$

In order to calculate them, we have to take all possible average values of AA and $\Psi\bar{\Psi}$. As a result, for $\langle \Psi(x) \bar{\Psi}(x') \rangle$ we will have the equation

$$\text{---} \leftarrow \times \text{---} = \begin{array}{c} x \quad x' \\ \diagup \quad \diagdown \\ y \quad y' \end{array} + \begin{array}{c} x \quad x' \\ \diagup \quad \diagdown \\ y \quad y' \end{array} + \begin{array}{c} x \quad x' \\ \diagup \quad \diagdown \\ y \quad y' \end{array} + \dots, \quad (5.7)$$

and a similar graphic equation for $\langle A(x) A(x') \rangle$. The functions corresponding to the vertical lines are now exact retarded Green's functions

$$\text{---} \leftarrow G_R = \text{---} \leftarrow G_R^0 + \text{---} \leftarrow \times \text{---} G_R^0 + \text{---} \leftarrow \times \text{---} D_R^0 + \dots \quad (5.8)$$

Let us see, what happens to (5.7) when $y_0 = t \rightarrow -\infty$. In a theory without confinement the answer is very simple. If the retarded Green's function has a pole at $p^2 = m^2$, the diagram

$$\begin{array}{c} x \quad x' \\ \diagup \quad \diagdown \\ y \quad y' \end{array} \quad (5.9)$$

has a finite limit when $y_0 \rightarrow -\infty$ and equals

$$\int dq_0 e^{-iq_0 \left(\frac{x_0 + x'_0}{2} - y_0 \right)} \int e^{ik(x-x')} \frac{d^4 k}{(2\pi)^2} \delta(k^2 - m^2) \delta((q-k)^2 - m^2) f(k), \quad (5.10)$$

where $f(k)$ corresponds to $\text{---} \leftarrow \times \text{---}$. The product of the δ -functions gives

$$\delta((q-k)^2 - m^2) \delta(k^2 - m^2) = \delta(k^2 - m^2) \delta(q_0^2 - 2k_0 q_0) \rightarrow \frac{\delta(k^2 - m^2)}{2k_0} \delta(q_0), \quad (5.11)$$

and therefore (5.10) does not depend on y_0 . For a free Green's function

$$\begin{array}{c} x \quad x' \\ \diagup \quad \diagdown \\ y \quad y' \end{array} = \text{---} \leftarrow \times \text{---} \quad (5.12)$$

and instead of (5.7), we have the usual relation for the imaginary part of the fermion Green's function

$$\text{---} \leftarrow \times \text{---} = \text{---} \leftarrow \times \text{---} + \text{---} \leftarrow \times \text{---} + \dots \quad (5.13)$$

Repeating the same calculation in a theory in which the Green's functions of quarks and gluons have no poles but soft singularities we will get $\langle \Psi(x) \bar{\Psi}(x') \rangle = 0$ in the $t \rightarrow -\infty$ limit. This, of course, cannot be the correct answer — in the theory with confinement there exist stable hadrons in general, and those belonging to the pseudoscalar octet in particular. The problem can be resolved by introducing these pseudoscalar particles from the very beginning as elementary objects [6]. In this case we include in the Dirac equation for Ψ not only the colour field A but also the pseudoscalar field φ . This will add to (5.7) diagrams of the form

$$(5.14)$$

where the wavy lines correspond to pseudoscalar particles; for the sake of simplicity, we shall call them pions. They satisfy the equality

$$(5.15)$$

Instead of (5.13), we have

$$(5.16)$$

and for the gluonic imaginary part, correspondingly,

$$(5.17)$$

The equation (5.16) differs essentially from (5.13). It contains no driving term (like f_0 in (5.13)); it is a non-linear but homogeneous equation. The equation (5.17) contains driving terms coming from fermions.

Let us consider in detail (5.16) in terms of the equation (4.10) for $f(p)$. We can write $f(p)$ in the form

$$f(p) = \vartheta(p^2) \{f_+(p) + f_-(p)\} + \vartheta(-p^2) f_{Eucl}(p), \quad (5.18)$$

where f_{\pm} are the contributions of positive and negative frequencies p_0 .

Let us first investigate the contributions of the functions f_+ and f_- to the first term in the right-hand side of (5.16). The function $f_+(p)$ gives the usual contribution to the

imaginary part of the quark Green's function coming from the intermediate [positive energy] π and quark (q_+) states. The contribution of $f_-(p)$ is very interesting because the signs of the particle energies in the intermediate states are different [π and a negative energy quark q_-]. The expression for this contribution (without the external legs) is

$$\Delta_{q_-, \pi} = g^2 \int \frac{d^4 q}{8\pi^2} [\hat{q} a_-(q^2) + b_-(q^2)] \vartheta(-q_0) \delta((p-q)^2 - \mu^2) \vartheta(p_0 - q_0). \quad (5.19)$$

Here g is the coupling constant connecting the π -meson to quarks; a_- and b_- are two invariant functions for the imaginary part of the quark Green's function.

In order to understand the structure of (5.19) let us consider the integrals

$$\begin{aligned} I_2(p, \kappa, \mu) &= \int \frac{d^4 q}{8\pi^2} \delta(q^2 - \kappa^2) \delta((p-q)^2 - \mu^2) \vartheta(-q_0) \vartheta(p_0 - q_0) \\ &= \frac{1}{4\pi} \frac{1}{p^2} \sqrt{[p^2 - (\kappa + \mu)^2][p^2 - (\kappa - \mu)^2]} \\ &\quad \times \vartheta(p^2) \vartheta((\kappa - \mu)^2 - p^2) \{ \vartheta(-p_0) \vartheta(\kappa - \mu) + \vartheta(p_0) \vartheta(\mu - \kappa) \} \end{aligned} \quad (5.20)$$

and

$$\begin{aligned} I_1(p, \kappa, \mu) &= \int \frac{d^4 q}{8\pi^2} \hat{q} \delta(q^2 - \kappa^2) \delta((p-q)^2 - \mu^2) \vartheta(-q_0) \vartheta(p_0 - q_0) \\ &= \frac{1}{4\pi} \frac{\hat{p}}{p^4} (p^2 + \kappa^2 - \mu^2) \sqrt{[(\kappa - \mu)^2 - p^2][(\kappa + \mu)^2 - p^2]} \\ &\quad \times \vartheta(p^2) \vartheta((\kappa - \mu)^2 - p^2) \{ \vartheta(-p_0) \vartheta(\kappa - \mu) + \vartheta(p_0) \vartheta(\mu - \kappa) \}. \end{aligned} \quad (5.21)$$

Hence,

$$\Delta_{q_-, \pi} = g^2 \int d\kappa^2 \{ a_-(\kappa^2) I_1(p, \kappa, \mu) + b_-(\kappa^2) I_2(p, \kappa, \mu) \}. \quad (5.22)$$

The structure of I_1 and I_2 implies that f_- on the right-hand side gives contributions to both f_- and f_+ on the left-hand side. The equations for f_- and f_+ can be written in the following way:

$$f_- = G_R \Delta_{q_-, \pi}^- \bar{G}_R + \dots \quad (5.23)$$

$$f_+ = G_R \Delta_{q_-, \pi}^+ \bar{G}_R + G_R \Delta_{q_+, \pi}^+ \bar{G}_R + \dots, \quad (5.24)$$

where $\Delta_{q_-, \pi}^-(p)$ and $\Delta_{q_-, \pi}^+(p)$,

$$\Delta_{q_-, \pi}^-(p) = g^2 \int_{(\mu + \sqrt{p^2})^2}^{\infty} d\kappa^2 [a_-(\kappa^2) I_1(p, \kappa, \mu) + b_-(\kappa^2) I_2(p, \kappa, \mu)] + \dots, \quad (5.25)$$

$$\begin{aligned} \Delta_{q_-, \pi}^+(p) &= g^2 \vartheta(\mu - \sqrt{p^2}) \\ &\quad \times \int_0^{(\mu - \sqrt{p^2})^2} d\kappa^2 [a_-(\kappa^2) I_1(p, \kappa, \mu) + b_-(\kappa^2) I_2(p, \kappa, \mu)] + \dots, \end{aligned} \quad (5.26)$$

are the contributions corresponding to the quark masses κ larger ($\kappa > \mu$) and smaller ($\kappa < \mu$) than the π -meson mass μ , respectively. Higher order terms have the same structure: large quark masses of f_- contribute to f_- , small quark masses contribute to f_+ .

Inserting this solution into the last term of (5.29) we will have an equation similar to (5.24) with the only difference that $\Delta_{q^-, \pi}^+$ in (5.24) acquires an additional contribution from multi-pion states. This will not change any of the conclusions we have reached, because it is only f_+ and f_- which matter for the calculation of the retarded Green's function.

The structure of f_{Eucl} written in (5.31) is, nevertheless, interesting in two respects. Firstly, it shows how the analytic features corresponding to Fig. 15 (with functions having discontinuities at positive and negative p^2 values) can be reduced to analytic features corresponding to Fig. 16 where the discontinuity differs from zero only at positive p^2 values. Secondly, the existence of the integrals in (5.31) imposes a restriction on $f_-(p)$.

References

- [1] V.N. Gribov, *Physica Scripta* **T 15** (1987), 164
- [2] Vladimir N. Gribov, Orsay lectures on confinement (II), LPTHE Orsay 94-20 (1994), hep-ph/9404332
- [3] V.N. Gribov, Lund preprint LU-TP 91-7 (1991)
- [4] F.E. Close, Yu.L. Dokshitzer, V.N. Gribov, V.A. Khoze, M.G. Ryskin, *Phys. Lett. B* **319** (1993), 291
- [5] V.N. Gribov, *Bound states of massless fermions as a source for new physics*, in Proceedings of the International School of Subnuclear Physics, 33th Course, Erice, Italy, 1995, ed. A. Zichichi, World Scientific, p. 1, Bonn preprint TK-95-35 (1995), hep-ph/9512352
- [6] V.N. Gribov, Bonn preprint TK-97-08 (1997), hep-ph/9807224 (annotated version)
- [7] V.N. Gribov, *The theory of quark confinement*, in Proceedings of the International School of Subnuclear Physics, 34th Course, Erice, Italy, 1996, ed. A. Zichichi, World Scientific, p. 30